







Optimized 12-Pulse Rectifier With Generalized Delta Connection Autotransformer and Isolated SEPIC Converters for Sinusoidal Input Line Current Imposition

Antônio de Oliveira Costa Neto , Ana Lúcia Soares , Gustavo Brito de Lima , Danillo Borges Rodrigues ,
Ernane Antônio Alves Coelho , and Luiz Carlos Gomes Freitas 

Abstract—This paper discusses an alternative to reduce harmonic current distortion in a 12-pulse rectifier. The circuit is based on a generalized autotransformer connection with low power-to-core that feeds two isolated SEPIC converters. Compared to other passive devices operating as conventional 12-pulse rectifiers, besides a tight dc bus, the use of static converters can, by means of an active current imposition, provide very low harmonic distortion of current. This paper presents a theoretical analysis which is corroborated by computational and experimental results. The results show that the performance of the proposed converter is similar to the performance provided by three-phase unity power factor PWM rectifiers, however, only two active switches are deployed.

Index Terms—AC/DC converter, autotransformer, harmonic, multipulse rectifiers, power factor correction, 12-pulse rectifiers.

I. INTRODUCTION

AS THE use of uninterruptible power supply systems and diverse sources of energy increases across a variety of different applications, the use of high power converters becomes ever more necessary. These in turn need to possess features of low weight and volume, as well as operate within the limits imposed by international standards [1], [2]. In order to decrease the harmful effects of nonlinear loads on these systems, different techniques are employed for correcting the power factor and

Manuscript received February 19, 2018; revised April 26, 2018; accepted June 14, 2018. Date of publication July 3, 2018; date of current version February 20, 2019. This work was supported by UFU, Capes, and CNPq (Under processes: 406845/2013-1, 304307/2013-0, 304252/2013-1, 301209/2010-3, and 420602/2016-0). Recommended for publication by Associate Editor J.-I. Itoh. (Corresponding author: Luiz Carlos Gomes Freitas.)

A. de O. C. Neto, A. L. Soares, G. B. de Lima, E. A. A. Coelho, and L. C. G. Freitas are with the Núcleo de Pesquisa em Eletrônica de Potência, Universidade Federal de Uberlândia, Faculdade de Engenharia Elétrica, Uberlândia 38400-902, Brazil (e-mail:

current. In these studies, noninsulated topologies are used [10] along with insulated [12], however, with a large quantity of semiconductor devices.

Recent studies that have used MPC structures with IPR's operating with static converters can be seen in [11], [14]–[18], where one has a current imposition that flows through the IPR's. This imposition results in sinusoidal currents on the electric energy grid. However, there does not exist any voltage regulation on the dc bus.

In light of the aforementioned, this study presents a 12-pulse rectifier with an autotransformer with a generalized connection and a differential delta topology supplied by two isolated SEPIC converters, as illustrated in Fig. 1. The main contributions of this study are highlighted through the following operational aspects.

- 1) In terms of the autotransformer used:
 - a) The galvanic insulation generated by SEPIC converter allows autotransformer applications in the input stage, thus the most part of power flow occurs by electrical conduction, with low power flow through the magnetic core. The connection, and the transformation ratio allow for low power processing in relation to the core of the autotransformer. In view of these features, a compact structure was obtained, with a reduced cost and weight.
- 2) In terms of the static converters used:
 - a) A reduced number of semiconductors, since only two SEPIC converters are used, as galvanic insulation eliminates the need for additional semiconductors that aid parallel connection at the output stage, as noted in [5], [9], and [10].
 - b) Dispenses the use of interphase transformers/reactors as a means of correcting instantaneous voltage differences between each rectifier group caused by lag between the transformer secondary voltages, thus reducing cost and increasing reliability.
- 3) In terms of the implemented control technique:
 - a) Output voltage regulation, which can be used in a number of applications, as for example in telecommunication sources, battery chargers and dc motor trigger systems.
 - b) High power factor and low total harmonic distortion of the input currents, in agreement with norm IEC 61000 3-2. Producing a better performance than conventional PWM rectifiers [13], [14], as with the 18 and 24-pulse rectifiers, however, with a lower cost autotransformer and a lower number of static converters and/or semiconductors.
 - c) As presented in [10] and [12], the use of the look-up-table as an alternative for generating triangular waveforms makes the system more susceptible to frequency variation on the ac grid, thus, compromising its performance when it comes to reducing current harmonic content. Through the control technique proposed in this study, these problems are solved by using digitally generated triangular references of the current that are in synchronism with the line voltage of each rectifier group.

II. OPERATION PRINCIPLES OF THE PROPOSED CONVERTER

A. Autotransformer With a Generalized Differential Delta Connection

The proposed rectifier consists of a structure with an autotransformer with a generalized differential delta connection, since one can easily alter the transformation ratio [3], [4]. Analogously to the conventional 12-pulse rectifier, the proposed rectifier possesses three primary windings and twelve auxiliary windings, as well as supplying, at its output, two systems that are out of three phase by 30° one from the other.

As noted on Fig. 1, the input currents are formed by the sum of the currents that circulate on the auxiliary windings of the respective phases and the current that flows through the delta windings, where k_b and k_c are the transformation ratios between the primary and auxiliary windings

$$i_{ab} = \frac{i_{c2} - i_{a1}}{k_b} + \frac{i_{b1} - i_{b2}}{k_c} \quad (1)$$

$$i_{bc} = \frac{i_{b2} - i_{c1}}{k_b} + \frac{i_{a1} - i_{a2}}{k_c} \quad (2)$$

$$i_{ca} = \frac{i_{a2} - i_{b1}}{k_b} + \frac{i_{c1} - i_{c2}}{k_c} \quad (3)$$

Being that

$$i_{a_{prim}} = i_{ca} - i_{ab} \quad (4)$$

$$i_{b_{prim}} = i_{bc} - i_{ca} \quad (5)$$

$$i_{c_{prim}} = i_{ab} - i_{bc} \quad (6)$$

Substituting (1) and (3) into (4)

$$i_{a_{prim}} = \frac{i_{a2} - i_{b1} - i_{c2} + i_{a1}}{k_b} + \frac{i_{c1} - i_{c2} - i_{b1} + i_{b2}}{k_c}$$

$$i_{b_{prim}} = \frac{i_{b2} - i_{c1} - i_{a2} + i_{b1}}{k_b} + \frac{i_{a1} - i_{a2} - i_{c1} + i_{c2}}{k_c}$$

$$i_{c_{prim}} = \frac{i_{c2} - i_{a1} - i_{b2} + i_{c1}}{k_b} + \frac{i_{b1} - i_{b2} - i_{a1} + i_{a2}}{k_c}.$$

B. Composition of the Input Currents

The adopted control technique is based on the imposition of triangular currents on the input inductors of each SEPIC converter. This should be in phase with the Vac line voltage of each group rectifier, as illustrated in Fig. 2. Thus, resulting in phase A from each rectifier group, for example, the waveform illustrated in Fig. 3 (currents i_{a1} and i_{a2}). Through the employment of the transformer, one has on the windings of phases AB and CA, the currents that contain the current drained from phase A of the ac supply grid, as illustrated in Fig. 3. Therefore, the conclusion is reached that the imposition of currents with triangular waveform and a frequency of 360 Hz on the input inductors of each SEPIC converter, opens the possibility for obtaining perfectly sinusoidal currents on the supply grid.

The control was implemented through algorithms in C language, using the digital controller TMS320F28335 from Texas Instruments. The methodology is divided into three main routines.

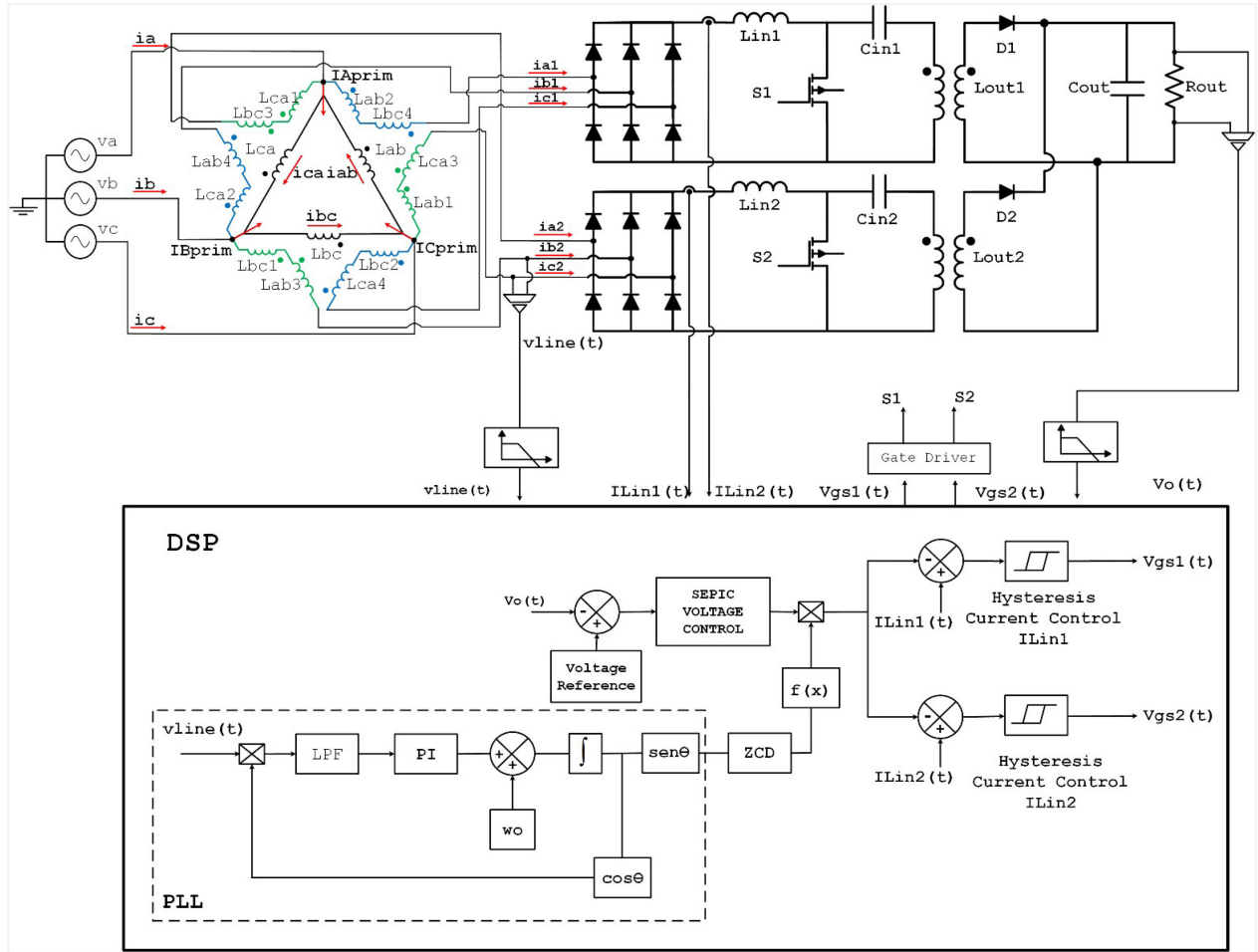


Fig. 1. Autotransformador Δ -diferencial com conversores SEPIC isolados.

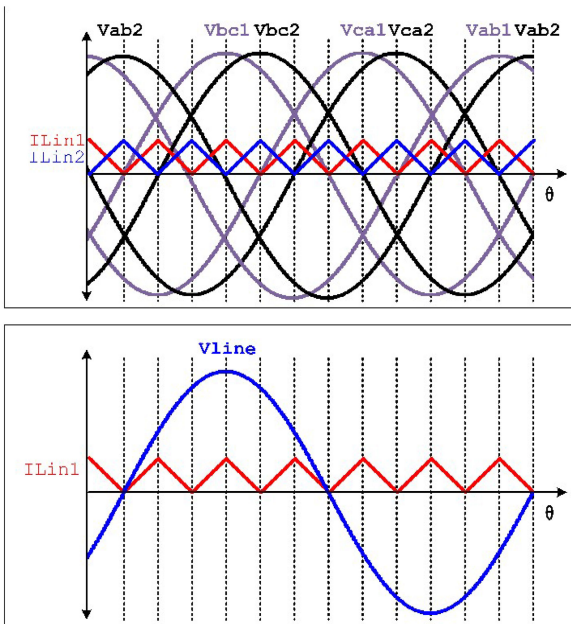


Fig. 2. Line voltage waveforms from the secondary of the autotransformer and the currents imposed at the input of each converter dc-dc.

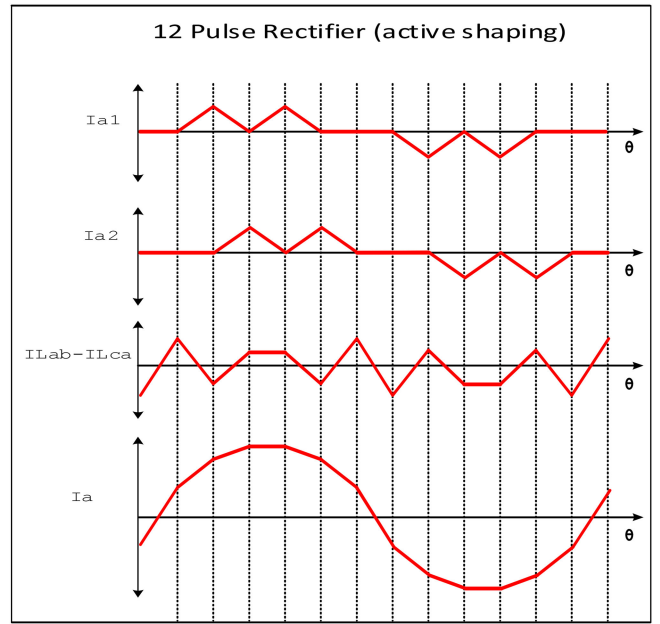


Fig. 3. Composition of theoretical waveforms—sinusoidal input current.

1) *Phase Locked Loop*: It is imperative that one of the line voltages on the ac side of each rectifier group is in phase with the current imposed on the input inductor of each SEPIC converter (see Fig. 3), to the contrary, one obtains current waveforms that are highly distorted. In order to solve this problem, a PLL algorithm (*phase locked loop*) is used.

2) *Zero Crossing Detector*: The output signal from the PLL passes through a zero crossing detector (ZCD), whose objective is to synchronize the PLL output in phase with the 360 Hz triangular waveforms generated through an equation, which is a function of the frequency variation read from the PLL output signal. The 360 Hz frequency is used keeping in mind that the currents drained from the ac grid are obtained through (7)–(9). Therefore, as a consequence, one obtains the ideal composition for the phase currents sinusoidal waveform and THD_i less than 5%. The signal from the ZCD ($f(x)$), is multiplied by the control voltage from the voltage compensator PI, thus generating the reference for the current imposed on each SEPIC converter

$$i_a = i_{a1} + i_{a2} + i_{ab} - i_{ca} \quad (7)$$

$$i_b = i_{b1} + i_{b2} + i_{bc} - i_{ab} \quad (8)$$

$$i_c = i_{c1} + i_{c2} + i_{ca} - i_{bc}. \quad (9)$$

3) *Average State-Space Model for Determining the Transfer Functions of the Plant and Voltage Controller*: The transfer function from SEPIC converter can be obtained through an analysis of average state space. With the data presented in Table I, the transfer function $G_{V_{out}/i_{in}}$ is given by (10). Therefore, the SISOTOOL from the software MATLAB was used to obtain the output voltage compensator and to analyze the performance of the internal voltage loop control. From the Tustin method, the discrete transference function is obtained in (11) and straight after, the different compensator equations is shown in (13). The Simulink tool from the software MATLAB was used to simulate the complete system in closed loop, as portrayed in Fig. 4, where one notes from the step response an overshoot around 10% and it comes into steady state at about 60 ms, which demonstrates that the voltage controller has a quick enough response to control the output voltage, as desired. It is important to emphasize that, in order to mitigate the output voltage oscillation, the voltage compensator was designed with an additional pole at 360 Hz and a sample rate frequency was established at 100 kHz. Fig. 5 presents the respective Root locus of the internal voltage loop proving the stability of the system (Gain Margin: 26 dB and Phase Margin: 69.6°)

$$G_{V_{out}/i_{in}} = \frac{a2 \cdot s^2 + a0}{b3 \cdot s^3 + b2 \cdot s^2 + b1 \cdot s + b0} \quad (10)$$

where

$$a2 = C_{in} \cdot L_{out} \cdot R_{out} - C_{in} \cdot D \cdot L_{out} \cdot R_{out}$$

$$a0 = D \cdot R_{out} - D^2 \cdot R_{out}$$

$$b3 = C_{in} \cdot C_{out} \cdot L_{out} \cdot R_{out}$$

TABLE I
PROJECT SPECIFICATIONS

Input Line Voltage	220Vrms
DC bus voltage	315Vcc
Efficiency	92%
THD _i	in accordance with IEC 61000 3-2
Autotransformer	
Input voltage	220V/60Hz – Three-phase
Rectified output voltage	2 x 300 Vcc
Power output	2.5 kW
Primarys: L _{AB} , L _{BC} , L _{CA}	19 AWG/977 coils
Auxiliaries 1 and 2: L _{AB1} , L _{AB2} , L _{BC1} , L _{BC2} , L _{CA1} , L _{CA2}	22 AWG/134 coils
Auxiliaries 3 and 4: L _{AB3} , L _{AB4} , L _{BC3} , L _{BC4} , L _{CA3} , L _{CA4}	22 AWG/23 coils
Core type	E – 1 M25 – 27 GO
Maximum Magnetic Flux Density	0.94T
Blade Thickness	0.27 mm
Core area	202.5 cm ²
Window area	22.5 cm
Stack height	3 cm
Tongue width	3 cm
Rectifying bridges	SKD35/12
SEPIC Converters	
Power output for each converter	500W
Maximum switching frequency	50kHz
Input inductance Lin1, Lin2	10mH
Magnetizing inductance Lout, Lout2	1mH
Input capacitance Cin1, Cin2	4.4μF
Output capacitance Cout	470μF
Average duty cycle	0.44
Switches S1 and S2	MOSFET C2M0080120D (36A/1200V)
Output Diode D1 and D2	RHRG30120 (30A / 1200V)

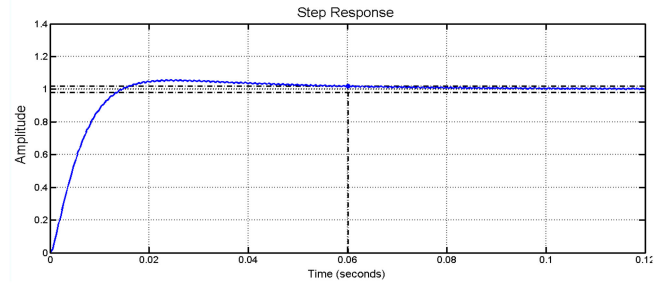


Fig. 4. Step response of the internal voltage loop.

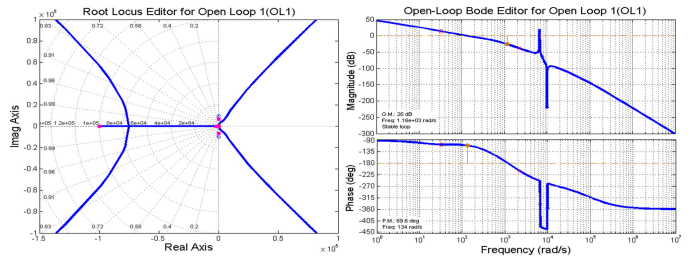


Fig. 5. Root locus of the internal voltage loop.

$$b2 = C_{in} \cdot L_{out}$$

$$b1 = C_{in} \cdot R_{out} - 2 \cdot C_{in} \cdot D \cdot R_{out} + C_{out} \cdot D^2 \cdot R_{out}$$

$$b0 = D^2$$

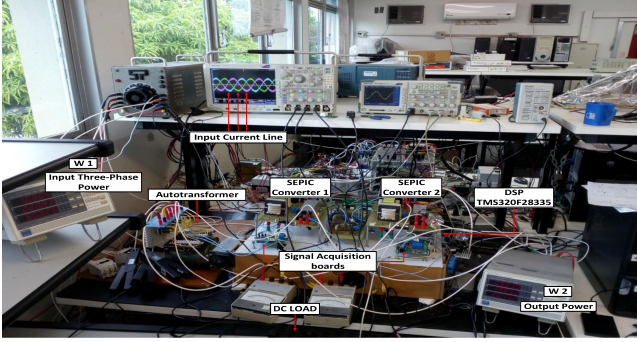


Fig. 6. Experimental setup overview view.

$$\frac{Kv(s)}{Ev(s)} = 0.05 \cdot \frac{0.03 \cdot s + 1}{0.03 \cdot s \cdot (s \cdot 0.00044 + 1)} \quad (11)$$

$$\frac{Kv(z)}{Ev(z)} = \frac{0.001724 \cdot z + 5.74 \cdot 10^{-7} - 0.0017 \cdot z^{-1}}{z - 1.9310 + 0.9310 \cdot z^{-1}} \quad (12)$$

$$Kv[k] = x1 + x2 + x3 + x4 + x5 \quad (13)$$

where

$$x1 = 1.9310 \cdot Kv[k - 1]$$

$$x2 = -0.9310 \cdot Kv[k - 2]$$

$$x3 = 0.0017 \cdot Ev[k]$$

$$x4 = 5.74 \cdot 10^{-7} \cdot Ev[k - 1]$$

$$x5 = -0.0017 \cdot Ev[k - 2]$$

Kv Transference functions of the voltage compensators.

Ev Error signal between the reference and the signal captured by the sensors.

k Present sample.

$k - 1$ Previous sample.

$k - 2$ Previous sample.

In order to control the input current for each SEPIC converter, the Hysteresis controller was employed, due to its speed and excellent dynamic performance for the wide range of load variation. In the current hysteresis loops, the same voltage compensator signal guarantees the balance between the currents with the aim of assuring the correct composition of the input currents. In the comparison of the feedback signal with the current reference signal, one obtains the command signals for the switches of the SEPIC converters. The switching frequency is therefore variable, arriving at a maximum of 50 kHz.

III. EXPERIMENTAL RESULTS

In pursuance of validating the strategy of the proposed control, computer simulations were performed using the software PSIM. To corroborate the obtained theoretical results, a prototype of 1 kW was developed and analyzed in the laboratory, as illustrated in Fig. 6. In Table I, the specifications of the implemented rectifier are presented.

Figs. 7–9 show the signals for the obtained input currents and their respective frequency spectrums for the nominal power condition. The individual harmonic components are compared to the limits imposed by norm IEC 61000 3-2, thus, demonstrating that the structure operates with a harmonic distortion of 2.81% on each phase. In Figs. 10 and 11, the experimental results are shown, these show the dynamic response of the output voltage controllers and input currents, when subjected to steps of $\pm 50\%$, thus, demonstrating a satisfactory behavior with respect to the output voltage, considering the variation of only 30 Volts during the transient period. In Fig. 12, the input current waveforms obtained with ordinary control strategy (12-pulse operation) is presented.

Fig. 13 shows the relationship between the voltage and current for the obtained phase, which prove that an almost unitary power factor was obtained. In Fig. 14, the secondary reference voltage is shown together with the input current for the same rectifier module, demonstrating PLL synchronization.

Finally, in Figs. 15–17, the THD_i graphs are presented for the input currents, concerning power factor and yield obtained in accordance with the power delivered to the load. Note there exists a clear improvement to the quality of the input currents and the power factor as the power output increases, which is due to the fact that the converter distances itself from the critical region of discontinuity. However, the global yield gradually decreases, while keeping in mind that the prototypes of the switching converters were designed for only 500 W each.

In conclusion, in Table II, a synthesis of the results is presented through a comparative study performed between the proposed structure and other important correlated works, which are of recent publication in specialized literature concerning the subject under study. The following criteria were taken into consideration: type of connection of the autotransformer used; kVA rate of the autotransformer; output voltage control; input current control; galvanic insulation; number of semiconductors; yield; THD_i ; and FP. Among the selected studies, the following are highlighted:

- 1) In [3]–[9], 18-pulse rectifiers are analyzed with different types of topology, from among those which provide a THD_i range of the order of 7%–13%.
- 2) In [10]–[18], 12-pulse structures are analyzed that operate through the injection of triangular currents on the output of each rectifier. Noted here is that the proposed technique, operating together with a 12-pulse autotransformer, was capable of reducing considerably the harmonic distortions from the input currents. This technique obtained better results than those obtained in 30-pulse rectifiers [13], [14], where a much higher quantity of rectifier groups are used. Noteworthy however, is that many of these structures make use of special transformers (IPT's, IPR's) and do not supply regulated voltage on the dc bus.

In light of the aforementioned, it should be noted that the proposed rectifier counts on an autotransformer designed with a kVA rate (nominal power of the autotransformer in relation to total output power) of 20.5%. If used as a 12-pulse rectifier, where the currents imposed on the switching converters are constant, this can be designed for 18.5%. By operating with

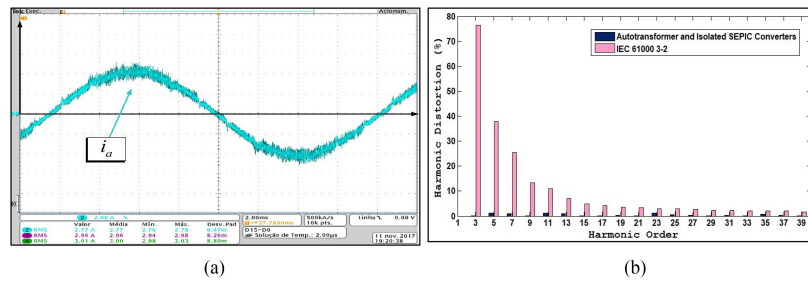


Fig. 7. (a) Input current of line A (2 A/div and 2 ms/div). (b) Harmonic spectrum of the input current in comparison with the harmonic content restrictions imposed by IEC 61000-3-2.

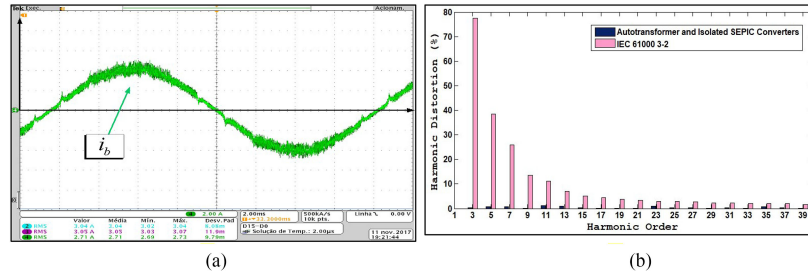


Fig. 8. (a) Input current of line B (2 A/div and 2 ms/div). (b) Harmonic spectrum of the input current in comparison with the harmonic content restrictions imposed by IEC 61000-3-2.

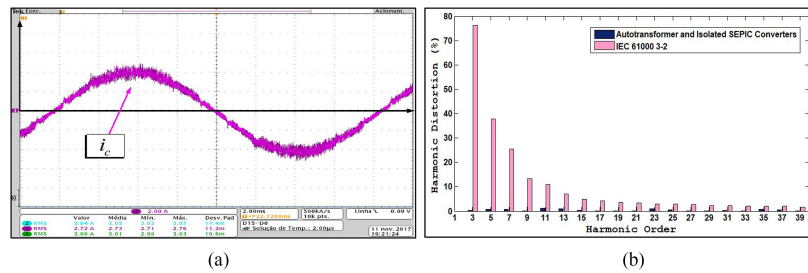


Fig. 9. (a) Input current of line C (2 A/div and 2 ms/div). (b) Harmonic spectrum of the input current in comparison with the harmonic content restrictions imposed by IEC 61000-3-2.

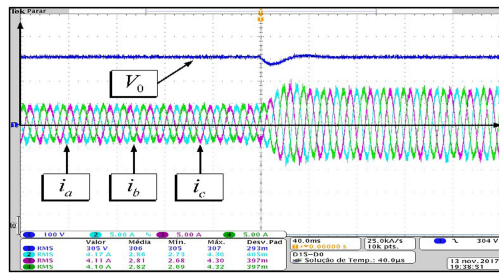


Fig. 10. Dynamic response during a load step-up from 1 to 2 kW (100 V/div, 5 A/div, and 40 ms/div).

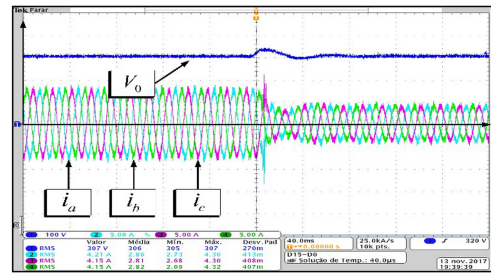


Fig. 11. Dynamic response during a load step-down from 1 to 2 kW (100 V/div, 5 A/div, and 40 ms/div).

triangular currents imposed on the input inductors of each switching converter, a THD_i of 3% was reached.

The delta-differential autotransformer with a generalized connection, although presenting a higher number of secondary windings—when compared to other autotransformer topologies presented in [3] and [4]—made the structure more compact in terms of the others, as it possesses a unitary transformation ratio. Highlighted also is that the voltage level adjustment on the

dc bus can be reached through the high frequency transformer of the switching converter, without affecting the increase of the kVA rate of the autotransformer. In addition, it promotes the galvanic insulation between the load and the ac grid.

The level of efficiency reached was similar to the other studies analyzed—around 92%—leaving only to highlight the reduced number of semiconductors used, which stimulates a reduction in costs and increases reliability.

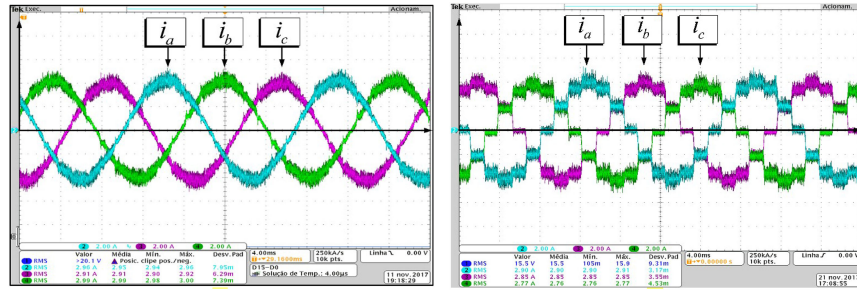


Fig. 12. Experimental results for the 1kW prototype in steady state ($V_{out} = 315\text{ V}$, $P_o = 1\text{ kW}$). (a) With active current imposition control – Sinusoidal current operation. (b) Without active current imposition control – 12-pulse operation. (2 A/div and 4 ms/div).

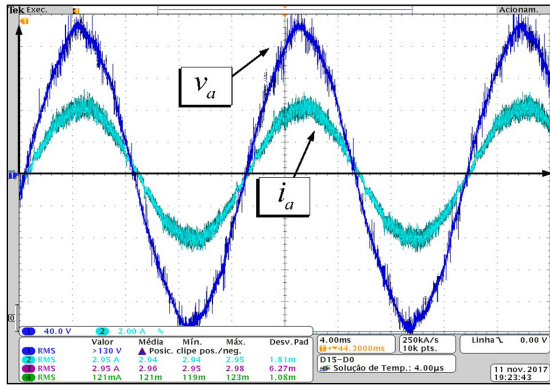


Fig. 13. Experimental results for the 1 kW prototype: Phase voltage and current multiplied by 50 ($V_{out} = 315\text{ V}$, $P_o = 1\text{ kW}$) (40 V/div, 2 A/div, and 4 ms/div).

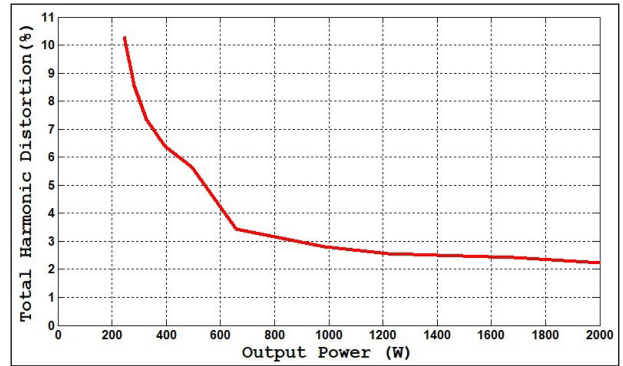


Fig. 15. Values of THDi as a function of the total output power.

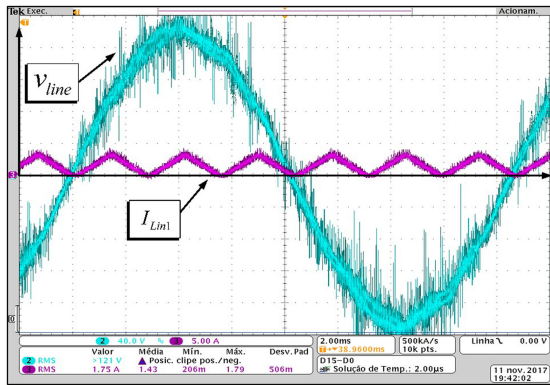


Fig. 14. Experimental results for the 1 kW prototype: Secondary line voltage synchronized with the input current for the inductor I_{Lin1} (40 V/div, 5 A/div and 2 ms/div).

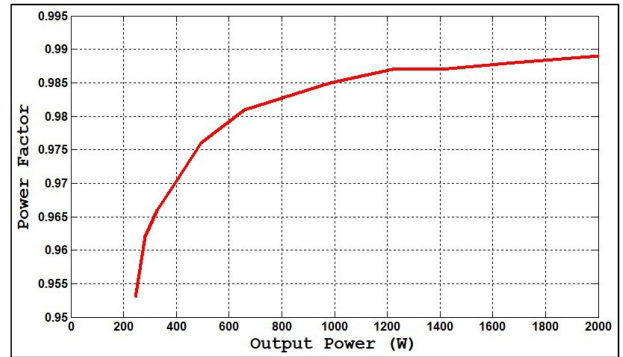


Fig. 16. Values of power factor as a function of the total output power.

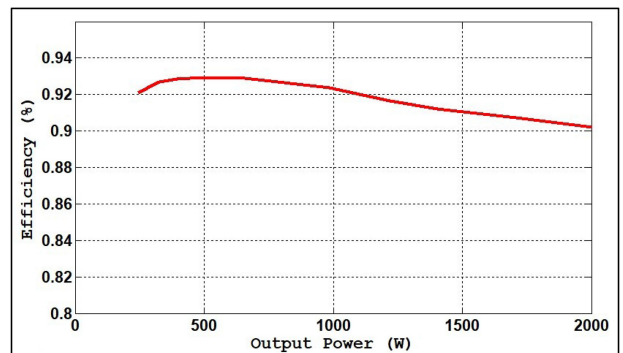


Fig. 17. Efficiency curves as a function of output power.

Noteworthy therefore is that the rectifier proposed in this paper presents important characteristics, which make it very attractive for applications as a preregulated stage in systems of up to 50 kW, including embedded electric energy generation systems, as for example those found in ships and airplanes—more electric aircrafts (MEA) [4], [8], [9]. In this context, it is noteworthy that the possibility of operating with a variable frequency on the ac supply side, since synchronism between the

TABLE II
COMPARISON BETWEEN RECTIFYING STRUCTURES OF MULTIPLE PULSES INCLUDING THE PROPOSED STRUCTURE

Developed Studies	Connection	Power Processing in relation to the core kVA (%)	Voltage regulation	Current Control	High Frequency Isolation	Number of Semiconductors (Switches/Diodes)	Power Output (kW)	Full Load Yield	THD _i %	PF
Autotransformer 18-pulse – IPT's [3]	Delta Differential	18	No	No	No	0 (0/0)	2.5	0.97	13	0.985
Autotransformer 18-pulse – BOOST [5]	Star Differential	22	Yes	Yes	No	9 (3/6)	12	0.94	8.8	0.99
Autotransformer 18-pulse – Full Bridge [6]	Star Differential	22	Yes	No	Yes	24 (12/12)	12	0.94	10.7	0.994
Autotransformer 18-pulse – Full Bridge [7]	Star Differential	22	Yes	No	Yes	24 (12/12)	12	0.9	8.6	0.99
Autotransformer 18-pulse – BOOST [8]	Delta Differential	28	No	Yes	No	9 (3/6)	6	0.93	7.8	0.992
Autotransformer 18-pulse – Sepic [9]	Delta Differential	18	Yes	No	No	9 (3/6)	2.4	0.92	8.4	0.994
Autotransformer 18-pulse – Sepic Isolated [9]	Delta Differential	18	Yes	No	Yes	6 (3/3)	2.4	0.9	7.2	0.994
Autotransformer 12-pulse – BOOST [10]	Delta Differential	24	Yes	Yes	No	6 (2/4)	-*	-*	2.7	-*
PROPOSED RECTIFIER Autotransformer 12-pulse – SEPIC Isolated	Delta Differential	20.5	Yes	Yes	Yes	4(2/2)	1	0.92	2.81	0.985
Autotransformer 12-pulse – IPR [11]	Delta Differential	18	No	Yes	No	4 (4/0)	-*	-*	Less than 1	-*
Autotransformer 12-pulse – Full Bridge [12]	Delta Differential	24	Yes	Yes	Yes	12 (8/4)	1.5	-*	2.7	-*
Autotransformer 12-pulse – PFC Converter [13]	Polygonal	38	No	No	No	8 (4/4)	55	-*	4.2	-*
Autotransformer 12-pulse IPR- Full Bridge [14]	Delta Differential	20	No	Yes	No	4 (4/0)	-*	-*	2.8	-*
Autotransformer 12-pulse IPR- BOOST [14]	Delta Differential	20	No	Yes	No	2 (1/1)	-*	-*	4.9	-*
Autotransformer 12-pulse Zig Zag - IPR [15]	Zig Zag	30	No	Yes	No	-*	6.25	-*	0.9	0.9995
Autotransformer 12-pulse Polygonal - IPT [16]	Polygonal	18	No	Yes	No	-*	1.5	-*	3.4	-*
Autotransformer 12-pulse – IPR [17]	Star	30	No	No	No	0 (0/0)	2	-*	3.9	-*
Autotransformer 12-pulse – IPR [18]	Delta	-*	No	Yes	No	-*	-*	-*	2.1	-*

* - Not mentioned by author/s.

currents imposed on the input inductors of switched converters and line voltage of the grid ensures correct composition of input currents, i.e., with THD_i less than 5%, as those obtained in conventional PWM converters.

IV. CONCLUSION

This paper provides an alternative for the improvement of harmonic distortions in 12-pulse rectifiers that use isolated SEPIC converters. A description of the autotransformer operation and the control strategy are presented. The study was validated through a computer and experimental analysis of a 1 kW prototype with results that conform to norm IEC 61000 3-2.

An important and insightful comparative analysis was presented taking into account the following consideration: Type of connection of the autotransformer used; kVA rate of the autotransformer; output voltage control; input current control; galvanic insulation; number of semiconductors; yield; THD_i; and PF. Among the selected studies, one can conclude that the proposed converter presents better results when compared to 18-pulses rectifiers and its performance is similar to the performance provided by three-phase unity power factor PWM rectifiers, however, only two active switches are deployed. Concerning the application range of the proposed structure, the authors highlight that in [13] a similar topology was tested on a 230 V, 75 hp motor drive system so reaching power levels

around 50 kW. One must also note that increasing the number of pulses of the autotransformer and hence increasing the number of SEPIC converters, despite splitting the rated power among three switched converters, would lead to the increase of the KVA rating of the autotransformer and of the costs, consequently.

In the light of these facts, the authors believe that only a careful efficiency and reliability analysis should be able to determine if the increase of costs can be justified. Concerning multipulse rectifiers, it is important to emphasize that the delta-differential autotransformer with a generalized connection, although presenting a higher number of secondary windings—when compared to other autotransformer topologies—made the structure more compact in terms of the others, as it possesses a unitary transformation ratio. Highlighted also is that the voltage level adjustment on the dc bus can be reached through the high frequency transformer of the SEPIC converter, without affecting the increase of the kVA rate of the low-frequency autotransformer. These in turn can be used in telecommunications, battery chargers, and in a wide range of industrial applications, as in the drive concepts of electric machines and applications involving MEA, where dc system are deployed for power distribution in order to reduce the weight, the size, and the losses, while increasing the levels of the transmitted power. To conclude, one must note that due to the ease of the control to adjust to frequency variations, there will be no problem to deploy the proposed structure in embedded systems, where they can operate together with permanent magnet generators.

REFERENCES

- [1] International Electrotechnical Commission, IEC-61000-3-2. Electromagnetic Compatibility (EMC)—Part 3-4: Limitation of Emission of Harmonic Currents in Low-voltage Power Supply Systems for equipment with Rated Current small than 16A, 1998.
- [2] IEEE, *IEEE Recommended Practices and Requirements for Harmonics Control in Electric Power Systems*, IEEE Standard 519, 1992.
- [3] P. S. Oliveira, F. J. M. Seixas, and L. S. C. e Silva, "A new design methodology for multipulse rectifiers with delta auto-connected transformers and a retrofit application in adjustable speed drives (ASDs)," in *Proc. IEEE IAS Annu. Meet.*, 2012, pp. 1–8.
- [4] R. C. Fernandes, P. S. Oliveira, and F. J. M. Seixas, "A family of auto-connected transformers for 12-and 18-Pulse Converters—Generalization for delta and Wye topologies," *IEEE Trans. Power Electron.*, vol. 26, no. 7, pp. 2065–2078, Jul. 2011.
- [5] F. J. M. Seixas and I. Barbi, "A new 12 kW three-phase 18-pulse high power factor AC-DC converter with regulated output voltage for rectifier units," in *Proc. 21st Int. Telecommun. Energy Conf.*, 1999, pp. 1–8.
- [6] F. J. M. Seixas and I. Barbi, "A new three-phase low THD power supply with high-frequency isolation and 60 V/200 A regulated DC output," in *Proc. IEEE 32nd Annu. Power Electron. Spec. Conf.*, 2001, pp. 1629–1634.
- [7] F. J. M. Seixas and I. Barbi, "A 12 kW Three-Phase Low THD Rectifier with High-Frequency isolation regulated DC Output," *IEEE Trans. Power Electron.*, vol. 19, no. 2, pp. 371–377, Mar. 2004.
- [8] R. C. Fernandes and F. J. M. Seixas, "AC-DC three-phase multipulse converter with boost DC-DC stage and constant hysteresis control," in *Proc. IEEE Brazilian Power Electron. Conf.*, 2011, pp. 403–408.
- [9] A. C. Lourenço, F. J. M. Seixas, J. C. Pelicer, and P. S. Oliveira, "18-pulse autotransformer rectifier unit using sepic converters for regulated dc-bus and high frequency isolation," in *Proc. IEEE 13th Brazilian Power Electron. Conf. 1st Southern Power Electron. Conf.*, 2015, pp. 1–6.
- [10] S. Choi, "A three-phase unity-power-factor diode rectifier with active input current shaping," *IEEE Trans. Ind. Electron.*, vol. 52, no. 6, pp. 1711–1714, Dec. 2005.
- [11] S. Choi, P. N. Enjeti, H. H. Lee, and I. J. Pitel, "A new active interphase reactor for 12-Pulse rectifiers provides clean power utility interface," *IEEE Trans. Ind. Appl.*, vol. 32, no. 6, pp. 1304–1311, Nov./Dec. 1996.
- [12] S. Choi and Y. Bae, "A new unity power factor telecom rectifier system by an active wave shaping technique," in *Proc. IEEE Ind. Appl. Conf.*, 2005, pp. 917–922.
- [13] M. M. Swamy, "An electronically isolated 12-Pulse autotransformer rectification scheme to improve input power factor and lower harmonic distortion in Variable-Frequency drives," *IEEE Trans. Ind. Appl.*, vol. 51, no. 5, pp. 3986–3994, Sep. 2015.
- [14] M. Anandpara, T. Panchal, and V. Patel, "An active inter-phase transformer for 12-Pulse rectifier system to get the performance Like 24-PULSe rectifier system," in *Proc. 18th Nat. Power Syst. Conf.*, Guwahati, India, Dec. 2014, pp. 1–6.
- [15] V. S. Vidyasagar, R. Kalpana, and B. Singh, "Improvement in harmonic reduction of zigzag autoconnected transformer based 12-Pulse diode bridge rectifier by current injection at DC side," in *Proc. IEEE Int. Conf. Power Electron., Drives Energy Syst.*, 2016, pp. 1–6.
- [16] M. Wang and F. Zhang, "12-pulse auto-transformer rectifier with harmonic current injection for non-grid-connected wind power applications," in *Proc. World Non-Grid-Connected Wind Power Energy Conf.*, 2009, pp. 1–5.
- [17] F. Meng, X. Xu, and L. Gao, "A simple harmonic reduction method in Multi-Pulse rectifier using passive devices," *IEEE Trans. Ind. Informat.*, vol. 13, no. 5, pp. 2680–2692, Oct. 2017.
- [18] F. Meng, L. Gao, S. Yang, and W. Yang, "Effect of single-phasing on multipulse rectifier with active interphase reactor," *IEEE Trans. Power Electron.*, vol. 30, no. 5, pp. 2549–2555, May 2015.
- [19] G. Gong, M. L. Heldwein, U. Drofenik, K. Mino, and J. W. Kolar, "Comparative evaluation of three-phase high power factor ac-dc converter concepts for application in future more electric aircrafts," in *Proc. IEEE Appl. Power Electron. Conf. Expo.*, 2004, pp. 1152–1159.
- [20] K. Mino, G. Gong, and J. W. Kolar, "Novel hybrid 12-pulse boost-type rectifier with controlled output voltage," *IEEE Trans. Aerosp. Electron. Syst.*, vol. 41, no. 3, pp. 1008–1018, Jul. 2005.
- [21] J. Chen, W. Chengjun, and C. Jie, "Investigation on the selection of a more suitable power system architecture for future more electric aircraft from the prospective of system stability," in *Proc. IEEE 26th Int. Symp. Ind. Electron.*, 2017, pp. 1861–1867.
- [22] L. A. Vitoi, J. A. Pomilio, and D. I. Brandão, "Analysis of 12-pulse diode rectifier operating in aircraft systems with constant frequency," in *Proc. IEEE Brazilian Power Electron. Conf.*, 2017, pp. 1–6.



Antônio de Oliveira Costa Neto was born in Uberlândia, Brazil, in 1992. He received the B.S. and M.Sc. degrees, in 2015 and 2018, respectively, in electrical engineering from the Universidade Federal de Uberlândia, Uberlândia, where he is currently working toward the Ph.D. degree in the Núcleo de Pesquisa em Eletrônica de Potência, Faculdade de Engenharia Elétrica.

His research interests include multipulse converters, digital control applied to power electronics, and power factor correction.



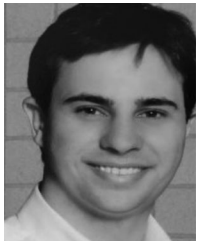
Ana Lúcia Soares was born in Bom Despacho, Minas Gerais, Brazil. She received the B.S. degree, in 2017, in electrical engineering from Universidade Federal de Uberlândia, Uberlândia, MG, Brazil, where she is currently working toward the M.S. degree.

Her research interests include power electronics, power factor correction, and multipulse transformer applications.



Gustavo Brito de Lima was born in Ibiassucê, Brazil, in 1986. Received the B.Sc., M.Sc., and Ph.D. degrees in electrical engineering from the Universidade Federal de Uberlândia, Uberlândia, MG, Brazil, in 2010, 2012, and 2015, respectively.

He is currently with NUPEP and since 2017 he has been a Professor Member. His research interests include hybrid rectifiers, digital control applied to power electronics, and power factor correction.



Danilo Borges Rodrigues was born in Uberlândia, Brazil, in 1986. He received the B.S. degree, in 2011, in electrical engineering from the Universidade Federal de Uberlândia, Uberlândia, where he is currently working toward the M.S. degree in the Núcleo de Pesquisa em Eletrônica de Potência, Faculdade de Engenharia Elétrica. His research interests include hybrid rectifiers, digital control applied to power electronics, and power factor correction.



Ernane Antônio Alves Coelho was born in Teófilo Otoni-MG, Brazil, in 1962. He received the B.Sc. degree in electrical engineering from the Universidade Federal de Minas Gerais, Belo Horizonte, Brazil, in 1987, the M.Sc. degree from the Universidade Federal de Santa Catarina, Florianópolis, Brazil, in 1989, and the Ph.D. degree from the Universidade Federal de Minas Gerais, Belo Horizonte, Brazil, in 2000.

He is currently with the Núcleo de Pesquisa em Eletrônica de Potência, Universidade Federal de Uberlândia, Uberlândia, Brazil, where since 2001, he has been a Professor Member. His research interests include parallel connection of pulsewidth modulated inverters, power factor correction, and digital control by microcontrollers and DSPs.



Luiz Carlos Gomes Freitas received the B.Sc., M.Sc., and Ph.D. degrees in electrical engineering from the Universidade Federal de Uberlândia, Uberlândia, MG, Brazil, in 2001, 2003, and 2006, respectively.

He is currently with NUPEP, where he has been working to establish research and education activities with regards to power electronics. His research interests include high-frequency power conversion, active power factor correction techniques, hybrid rectifiers, power quality, clean power applications, power electronics converters, and control technique for renewable energies sources-based systems and microgrids.

Dr. Freitas received the Prize Paper Award from IEEE-IAS-Industrial Automation and Control Committee for his contribution at the Hybrid Rectifiers field in 2012. He is a Member of the Brazilian Society of Power Electronics and a Member of NUPEP since 2008.